Green protectives on corroded copper artworks: Surface characterization and electrochemical behaviour in simulated acid rain

Margherita Donnici, Erika Ferrari, Delphine D. Neff, Salvatore Daniele

Green protectives on corroded copper artworks: surface characterization and electrochemical behaviour in simulated acid rain

Margherita Donnici[a], Erika Ferrari[b], Delphine Neff[b]*, Salvatore Daniele[a]*

[a] Department of Molecular Sciences and Nanosystems, University Ca' Foscari Venice,

Via Torino 155, 30137, Venice, Italy.

[b] NIMBE-LAPA, CEA, CNRS, Université Paris-Saclay, CEA Saclay, 91191 Gif-sur-Yvette, France.

* corresponding authors:

Orcid: 0000-0003-0315-1819

E-mail address: sig@unive.it

Tel: + 39 0412348630

E-mail address: delphine.neff@cea.fr

Abstract

The protective effects of decanoic acid (HC10) and sodium decanoate on naturally corroded copper-based artworks in synthetic acid rain (pH 3.1) were evaluated and compared to those of benzotriazole (BTA). Surface characterization (by colorimetry, optical microscopy, SEM, contact angle and Raman spectroscopy) was coupled with open circuit potential and potentiodynamic measurements. The samples used were copper cladding from the roof of St Martin's Church in Metz (France) and, for comparison, bare copper specimens. This study demonstrated that HC10 may represent an eco-friendly and efficient alternative to the use of BTA for maintaining the naturally formed patinas of copper-based artworks exposed outdoors.

Keywords: Copper artworks; Corrosion inhibitors; Decanoic acid; Sodium decanoate; Acid rain; Hydrophobic layer.

1. Introduction

Metals exposed to urban environments undergo corrosion processes, which lead to extensive changes in their chemical composition, physical structure and, hence, aesthetic appearance [1, 2]. In the case of copper, which was widely used for architecture in the past, its corrosion leads to the formation of corrosion layers whose characteristics depend on the reactivity of the species present in the environment. Previous studies have shown that when copper is exposed to an urban environment for a significant amount of time, corrosion layers form that are essentially composed of an inner layer of cuprite (Cu_2O), typically 5-10 µm thick, and a green external layer of brochantite ($Cu_4SO_4(OH)_6$), typically 45-50 µm thick [3-5]. The latter, often displays great porosity and poor adhesion to the underlying cuprite layer [3]. In the field of conservation of historical and artistic materials, it is common practice to keep the corrosion layer (the so-called patina, naturally formed), unless it compromises the stability of the object. In fact, the patina provides evidence of the passage of time and adds historical value to the objects. Its color (usually green for copper materials) is aesthetically pleasing and it protects, to a certain extent, the underlying metal from further corrosive processes [4]. However, changes in the environmental conditions may cause destabilization of the corrosion layers leading to deterioration of the underlying metal. This is the reason why different strategies are adopted for the protection of metallic artifacts exposed outdoors. Among these strategies, the most common is the application of a protective organic coating, acting as a physical barrier between the object and the environment, based on either microcrystalline wax or acrylic resins [6]. In recent studies on patinated bronze, the use of new coating materials such as organosilanes [7,] and fluoropolymers [8] has also been proposed. In addition to the above types of coatings, corrosion inhibitors have traditionally been employed for conservation in the form of lacquers, like for instance, Incralac®, a blend of acrylic resins which, among other components, also contains benzotriazole as UV stabilizer and, possibly, as

suggested in [9], as corrosion inhibitor. Alternatively, a corrosion inhibitor solution can be used before applying a protective organic coating [10].

For copper-based materials, the most widely used inhibitor is benzotriazole (BTA), which has long been considered to be the reference corrosion inhibitor [11]. Its use in the field of conservation of archaeological and historical copper-based objects dates back to the 1960s [9]. However, since BTA is thought to be toxic (because of the aromatic moiety in the molecule) and to have carcinogenic effects [12], its use is now discouraged. Thus, in recent decades, interest in alternative, sustainable and harmless inhibitors for cultural heritage materials has substantially increased [13-15].

Among various emerging classes of compounds, linear carboxylate derivatives of fatty acids, extracted from vegetable oils, have received increasing attention [13-15]. These compounds have mainly been tested as corrosion inhibitors on bare or etched metals [14]. More recently, decanoic acid (HC10) has been studied as a treatment to prevent further corrosion of naturally corroded copper objects [15]. The protective effects of HC10 have been explained as being due to the formation of a water-insoluble layer of copper decanoate on and within the external patina. This information has been gathered by using spectroscopic and scanning auger microscopy techniques [16]. For corrosion studies and corrosion mechanism investigations, electrochemical techniques could provide additional information, in particular, about the redox activity of the materials. Therefore, this study presents the first comprehensive examination of the inhibition effects of HC10, its sodium salt, sodium decanoate (NaC10), and, for comparison, BTA on naturally corroded copper cladding from the roof of St Martin's Church in Metz (France). The surface modifications (color, contact angle, morphology, chemical structure) after each treatment were assessed by a set of complementary spectroscopic and surface analysis techniques, while the electrochemical properties and efficiency of the treatments were investigated by open circuit potential (OCP) and potentiodynamic polarization (PDP) measurements in a synthetic acid rain solution.

2. Research Aim

The aim of this study is to examine the protective effects of the green compounds decanoic acid and sodium decanoate, as alternatives to benzotriazole (whose use is now discouraged for its toxic properties), against further corrosion phenomena of the patina layer and the underlying metal of naturally corroded copper cladding from the roof of St Martin's Church in Metz (France). The patina is typically composed of cuprite and a green external layer of brochantite. In the field of conservation of historical and artistic materials, it is common practice to keep the corrosion layer, as it provides evidence of the passage of time and adds historical value to the objects. The study is specifically devoted to assess the surface modifications of the samples (color, contact angle, morphology, and chemical structure), following their treatment with the inhibitors, and the stability of the samples against further corrosion when they are exposed to a synthetic acid rain solution. To acquire this information, a set of complementary spectroscopic, surface analysis techniques and electrochemical measurements are employed.

3. Material and methods

3.1 Chemicals and solutions

All chemicals were reagent-grade (purity ≥95%), provided by Aldrich and used as received. The chemical structures of the three corrosion inhibitors employed are shown in Figure 1. The synthetic acid rain solution at pH 3.1, simulating the typical composition of rain in an urban environment [17], was composed of: H_2SO_4 0.325 mM (31.85 mg/l); HNO_3 0.25 mM (15.75 mg/l); NaCl 1.452 mM (84.85 mg/l); $NaNO_3$ 0.25 mM (21.25 mg/l); Na_2SO_4 0.225 mM (31.95 mg/l); and $(NH_4)_2SO_4$ 0.325 mM (46.20 mg/l) (see also Table S1). Bare copper sheet (99%) was provided by Alfa Aesar. All

aqueous solutions and the 50% (v/v) aqueous/ethanol mixtures were prepared using Milli-Q water (18.2MΩ·cm).

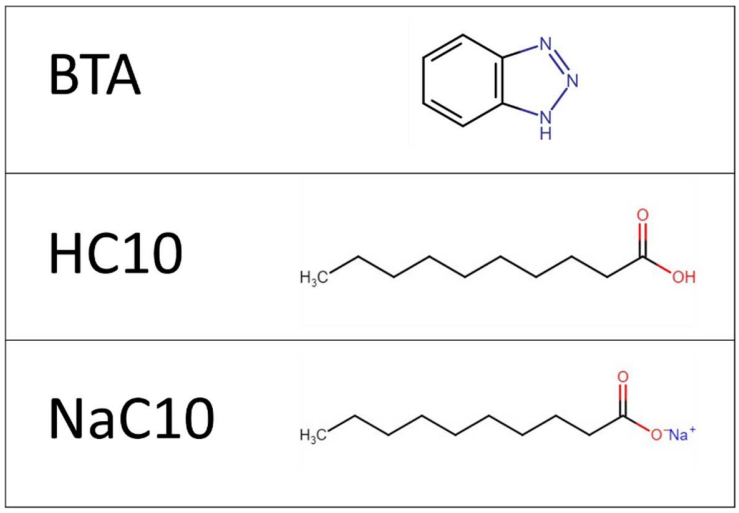

Figure 1: Chemical structures of benzotriazole (BTA), decanoic acid (HC10) and sodium decanoate (NaC10).

3.2 Sample preparation and treatments

Bare copper samples (about 1×1 cm^2) were cut from a 1mm thick copper sheet. The electric contact was made on one side by welding a copper wire with tin. Epoxy resin was used to embed the samples in order to expose only the non-welded sides of the samples to the solutions. The latter were then polished using successive abrasive SiC papers with 500, 800, 1200, 2000, and 4000 grit. They were then rinsed with deionized water and degreased with ethanol right before each experiment. The samples were then checked under an optical mycroscope to verify that no crevices between the edges of the sample and epoxy resin were formed. Only those samples that did not display such kind of defects were considered for further tests.

Samples of naturally corroded copper having a surface of ca. 1×1 cm^2 were cut from a larger copper plate (Figure 2). The plate, originally part of the roof cladding of St Martin's Church in Metz (France), had undergone long-term (>100 years) atmospheric corrosion. The side exposed to the atmosphere was easily distinguishable by the characteristic pale green corrosion layer (Figure 2a).

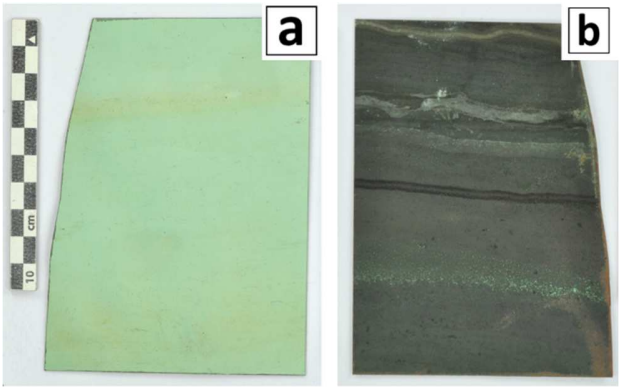

Figure 2: Top view of the corroded copper roof cladding from St Martin's Church in Metz. Upper side (a) and back side (b).

The surface of the samples was first cleaned with deionized water to eliminate powdery particles and then dried under ambient conditions. The side not exposed to the atmosphere (Figure 2b) was polished using SiC 500 grit paper and an electrical contact was made by soldering a copper wire with tin. Finally, both the electric contact and the reverse exposed surfaces were insulated by using a commercial nail varnish. Each type of sample to be examined was prepared in triplicate.

Treatment of the samples with the various inhibitors was performed in the 50%(v/v) water/ethanol medium containing: 0.25 M BTA, or 0.17 M HC10, or 0.15 M NaC10. These were the concentrations typically used in previous studies for cultural heritage artworks [15, 18, 19].

The samples were soaked in the inhibiting media for two hours and then air dried for 10-20 minutes prior to analysis. The efficiency of each treatment was evaluated after 24 hours of immersion, according to the study reported in the literature in the synthetic acid rain solution [14].

3.3 Surface characterization by non-electrochemical measurements on naturally corroded samples

Considering the relevance of the aesthetic impact of a treatment in the field of conservation, colorimetric analyses were performed on the naturally corroded samples by using a portable Minolta CM-2300d spectrophotometer coupled with SpectraMagic NX software. Colorimetric measurements on three samples for each treatment were performed. Reflectance spectra were collected between 360 nm and 740 nm using a standard D65 illuminant / 10° degrees observer angle. An auto average of five flashes on a spot of 8 mm diameter was recorded for each series of measurements. Data obtained were computed from the reflectance spectra and expressed in the CIEL*a*b* color space [20]; the color difference (ΔE) between untreated and treated samples was calculated as:

$$\Delta E = \sqrt{(\Delta L^*)^2 + (\Delta a^*)^2 + (\Delta b^*)^2} \qquad (1)$$

where ΔL^*, Δa^* and Δb^* represent the differences for each color parameter (L*, a*, b*) before and after treatment with the various inhibitors.

Changes in surface morphology due to the different treatments were evaluated by optical microscopy and scanning electron microscopy (SEM). Optical observations were made using an Olympus Light microscope with 5×, 10×, 20×, and 50× magnification lenses in bright field mode, while SEM images were obtained with a JEOL JSM-7001F scanning electron microscope. The micrographs were taken using an incident beam of 5 keV at a working distance of 4-6 mm. EDS analysis was performed only on the surface of the sample treated with sodium decanoate, using an acceleration voltage of 2 keV at a working distance of 10 mm. To avoid charging phenomena, the sample was coated with a carbon film.

The change in surface tension after each treatment was evaluated by the sessile drop method. For this purpose, a OCA20 Dataphysics Instruments tensiometer equipped with SCA20 software was employed. A drop of 5 μL of distilled water was placed on the surface and the contact angle was

measured after 10 seconds. Each contact angle value reported here, with relevant standard deviation, refers to the average obtained from 5 drops.

The impact of the treatments on the chemical structure of the sample surfaces was evaluated by performing μRaman spectroscopy. Spectra were collected using a Renishaw Invia Reflex, UK, spectrometer, equipped with a 532 nm Nd:YAG laser and CCD detector and coupled with an optical microscope. The spectra were recorded using a 50× objective and a laser power lower than 100 μW to avoid phase transformation by heating. The spot size examined by the spectrometer was 1 μm diameter and the spectral resolution was 2 cm^{-1}. Spectral calibration was performed using the main peak of a silicon wafer at 520.5 cm^{-1}. Spectra were processed using Wire 3.4 software and are presented here with no baseline correction.

3.4 Electrochemical measurements on uncorroded and naturally corroded copper samples

Open circuit potential and potentiodynamic polarization measurements were performed on the naturally corroded samples and, for comparison, on bare copper specimens, both untreated and treated with the different inhibitors.

A Bio-Logic Science Instrument potentiostat (Mod. SP-200), controlled by EC-Lab® software, using an electrochemical cell in a three-electrode configuration was employed. The copper samples were used as working electrodes; a platinum spiral (0.6/250mm) and an Ag|AgCl|KCl (3M) were employed as counter and reference electrodes, respectively. In all cases, the electrochemical tests were performed in the synthetic acid rain solution. Before PDP measurements, all samples were soaked in the solution and the OCP was measured for about 1 h, during which the potential reached a constant value (within ± 5 mV). PDP measurements were performed over the range of ±150 mV with respect to OCP, at 1 mV s^{-1}. All tests were performed in aerated solutions without stirring.

The corrosion inhibition efficiency was determined according to the following equation [14]:

$$IE\% = [(I_{corrUT} - I_{corrINH}) / I_{corrUT}] \cdot 100 \quad (2)$$

where I_{corrUT} and $I_{corrINH}$ are the corrosion current densities of the untreated and treated samples, respectively.

4. Results

4.1 Surface characterization by non-electrochemical methods

In order to understand the impact of the various treatments on historical materials the surface analyses reported below focused only on the naturally corroded samples (both untreated and treated with the inhibitors) of copper cladding from St Martin's Church in Metz (France).

4.1.1 Color change

Colorimetric parameter data (L*, a*, b*) and global color changes (ΔE*) were computed using the color of the uncoated sample as the reference. Results of the color measurements, obtained on three different spots on each sample treated with the inhibitor, before and after treatment, are summarized in Table 1.

Table 1: Color measurements on the naturally corroded samples before and after each treatment. The SCI (specular component included) values are also given.

Inhibitor	Sample	L*(SCI)	a*(SCI)	b*(SCI)	ΔE
BTA	untreated	72.2±1.5	-12.5±0.6	13.8±0.7	-
	treated	**59.4±0.4**	**-18.0±0.6**	**16.1±0.2**	**14.1±1.5**
HC10	Untreated	72.0±0.6	-12.1±0.4	14.2±1	-
	treated	**65.5±0.6**	**-24.2±09**	**4.8±05**	**16.7±1.4**
NaC10	untreated	72.2±1.5	-12.5±0.6	13.8±0.7	-
	treated	**70.5±1.2**	**-13±0.7**	**6.2±1**	**7.6±0.9**

As displayed in Table 1, the data confirm that the color of the untreated sample was uniform, as the values of L*, a* and b* parameters of the untreated samples are similar. After treatment with the inhibitors, all samples showed a change in color ($\Delta E > 0$). For the NaC10-treated sample, ΔE was the lowest, nevertheless appreciable to human eye. The parameters a* and b* decreased, while lightness (L*) remained unchanged, resulting in a slight whitening of the surface overall.

Treatments both with BTA and HC10 caused an appreciable change in the color of the samples, ΔE being equal to 14.1 and 16.7, respectively. In the case of BTA, the decrease of the L* value reflected a shift in color towards dark-green, in agreement with observations reported in the literature [21]. As for HC10, the decrease of the b* value reflected a color shift towards a blue hue.

4.1.2 Surface morphology

When observed under an optical microscope (Figure 3), the untreated surface was characterized by the presence of craters of about 30 µm diameter, a phenomenon previously observed on other historical copper roof cladding [5]; red and black stains were also visible. The stains may be due to external contamination incorporated into the surface. Both craters and stains were observed in the treated samples as well. The HC10-treated sample had a non-uniform surface with patchy-colored zones.

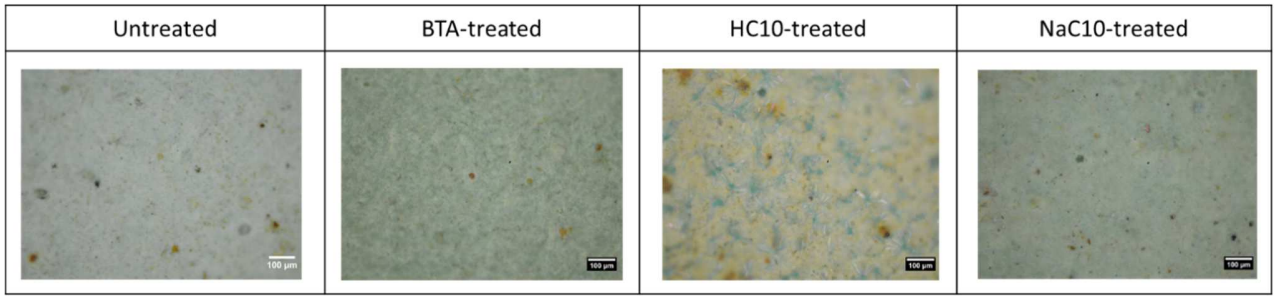

Figure3: Surface images obtained under an optical microscope (100×, bright field) of the naturally corroded samples, before and after treatment with inhibitors, as indicated.

In order to qualify the change in surface morphology at a higher magnification, SEM micrographs were taken in secondary electron mode. Figure 4 shows the main morphological modifications of the untreated (Figure 4a) and treated surfaces (Figure 4b-c).

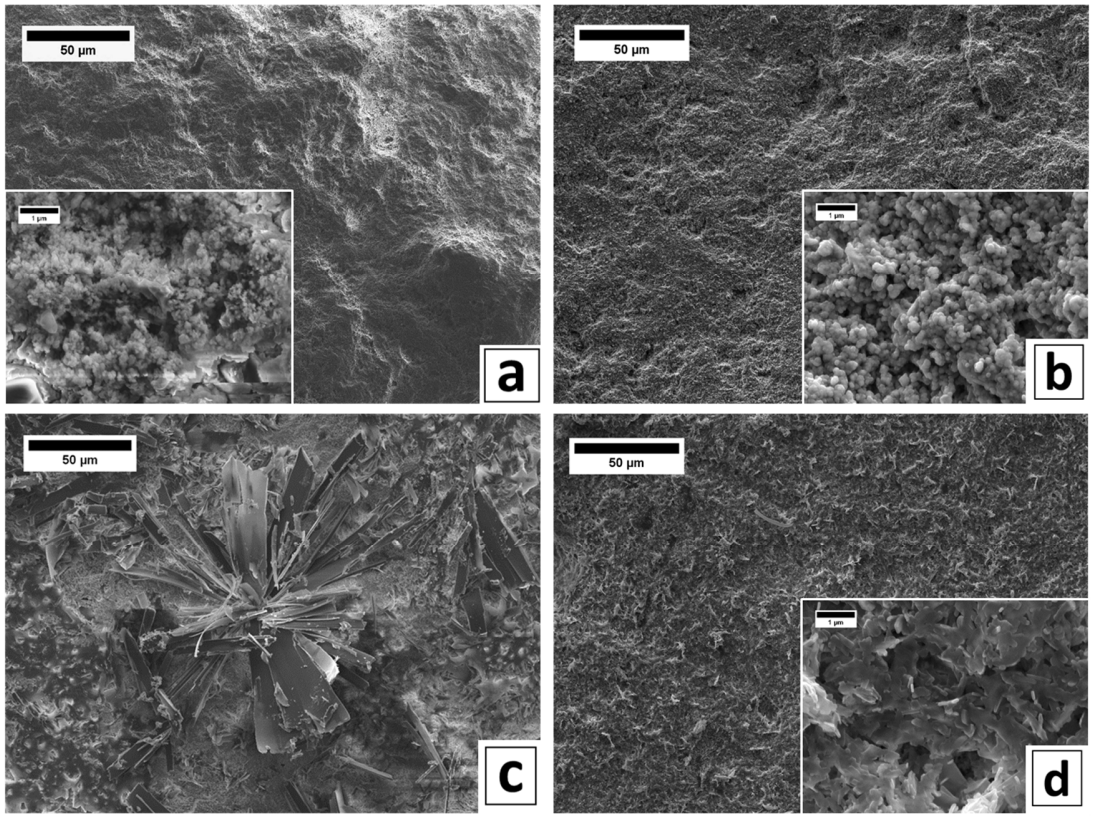

Figure 4: Secondary electron images of the surfaces of: (a) Untreated sample; (b) BTA-treated sample; (c) HC10-treated sample and (d) NaC10-treated sample.

The untreated surface (Figure 4a) appeared covered by powdery aggregates (diameter <0.1µm). The BTA-treated sample showed well defined round-shaped aggregates (Figure 4b). On the contrary, important morphological modifications were observed on the sample treated with decanoic acid. Large elongated crystals forming flower-like clusters could be clearly recognized on the surface (Figure 4c). Such morphology was observed in previous studies on bare copper treated with long-chain carboxylic acids [22]. The distribution of the crystals was not uniform across the surface; crystals were more

abundant in some areas. In the case of the NaC10 treatment, the surface morphology was heavily modified (Figure 4d). In fact, the surface was uniformly covered by irregularly-shaped, flake-like particles of homogeneous size (50-100 nm).

From optical microscope and SEM observations, it appeared that the surface morphology was most affected when the corroded samples were treated with HC10 and NaC10.

4.1.3 Contact angle

The results of the contact angle measurements are summarized in Figure 5. The value of the contact angle of the untreated sample was around 20°. This value, apart from being small, was somewhat uncertain, due to the quick change of the drop volume occurring in the first 10 seconds. This was due to the hydrophilicity of the surface. For the treated samples, stable contact angles of higher than 90° were

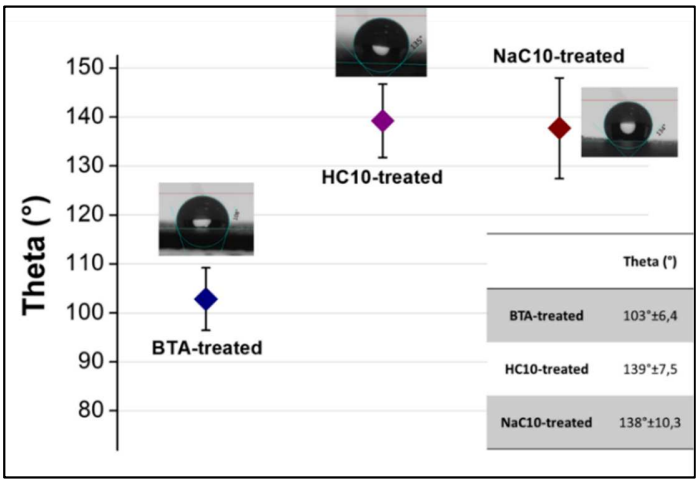

Figure 5: Contact angle measurements on the treated samples.

found in all cases. These results indicated that a hydrophobic layer formed on the sample surfaces after treatment with the three inhibitors. Interestingly, for the HC10- and NaC10-treated samples, the contact angles were close to 150°, the value typically observed for super-hydrophobic surfaces [23].

4.1.4 Structural characterization of the sample surface

The surface structural characterization of the various samples was performed by Raman spectroscopy (Figure 6). As expected, the main mineral phase found on the untreated sample (Figure 6a) was brochantite. This was inferred by the strong peak corresponding to the stretching of the SO_4^{2-} group at 973 cm^{-1} and the peaks due to -OH at 3587 cm^{-1} and 3563 cm^{-1} [24]; for comparison, a spectrum obtained from a specimen of reference brochantite is reported here (Figure 6a, red line).

The Raman spectra corresponding to the surface of the samples treated with the inhibitors are displayed in Figure 6b-d, which also include, for comparison, the reference spectra of the corresponding pure inhibitors. It must be noted that the band at 973 cm^{-1}, corresponding to the νSO_4^{2-}, denotes the predominant presence of brochantite in all samples which is the most stable mineral phase on copper materials exposed for long time to urban environments [25]. Since Raman spectra only provide information of the surface characteristics, no conclusion can be drown on how in depth this condition applies within the patina layer. However, in a previous work performed on corroded copper samples treated with BTA, it was shown that brochantite was present throughout the outermost patina layer [26].

Regarding the BTA-treated sample (Figure 6b, black line), the reactivity of BTA on the surface chemistry was indicated by several differences in band positions when comparing the spectra of pure BTA and the BTA-treated sample. For the latter, there was a notable absence of the -NH in plane bending mode at 1096 cm^{-1}, which is present in the spectrum of the pure BTA (Figure 6b, red line). This suggested that the –NH group interacted with species present on the sample surface to form, conceivably, the strong N-Cu chemical bond [27]. Other differences include the shift to higher

wavenumbers of several bands observed in the spectrum on the treated sample as compared to the reference BTA spectrum. Indeed, the benzene ring breathing mode at 781 cm^{-1} in pure BTA shifted to 790 cm^{-1} on the sample surface and the strong composite band at 1386 cm^{-1} shifted to 1395 cm^{-1} [28]. In addition, the latter bands were broader, compared to those of pure BTA, indicating a lower crystallinity of the material formed on the sample surface [28]. The latter findings also suggested an interaction between Cu(II) species and the N1 atom in benzotriazole to form a Cu-BTA complex (either amorphous or having lower crystallinity compared to solid BTA) on the sample surface, likely mixed with brochantite, according to a previous study [26].

Concerning the sample treated with HC10, the Raman spectrum (Figure 6c, black line), recorded specifically on the flower-like clusters observed by SEM (Figure 4c), provided all the ν(Cu-O) modes at 236 cm^{-1}, 288 cm^{-1} and 400 cm^{-1}, which confirmed the presence of copper decanoate [29] on the sample surface (Figure 6c, blue line).

Controversial information was obtained from the Raman spectra of the sample treated with NaC10 (Figure 6d, black line). In fact, the band at 288 cm^{-1}, one of the bands that identifies copper decanoate, was generally weaker with respect to the HC10-treated sample (Figure 6c, black line) and only clearly discernible in localized spots. The presence of $\nu(CH_2)$ at high wavenumbers and, in particular, the band at 2881 cm^{-1} indicated that a decanoate-type compound was present throughout the sample surface. To shed light on this aspect, EDS analysis was performed on the NaC10-treated surface using a low acceleration voltage (2 keV) in order to differentiate the Na Kα (1.04 eV) from the Cu Lα (0.9 eV). From these analyses, a sodium peak was detected on the EDS spectrum, which suggests the presence of some unreacted NaC10 (Figure S1). This can be due to the fact that NaC10, compared to the other inhibitors, could involve a slower chemical reaction, which would require longer immersion times to be completed.

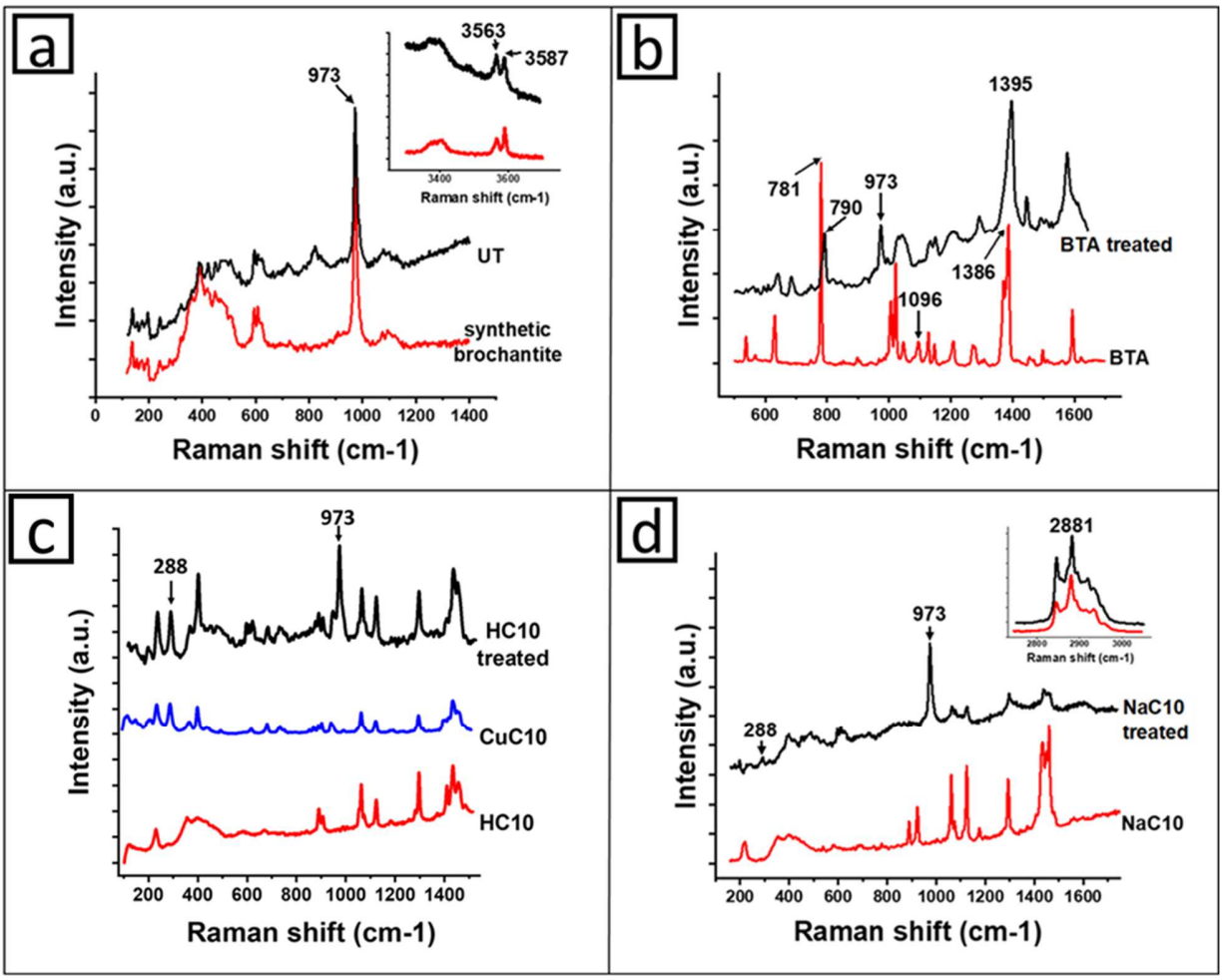

Figure 6: Raman spectra recorded on the surface of the samples: a) untreated and treated with b) BTA, c) HC10 and d) NaC10. The lines in black refer to the sample surface; the line in red refers to the corresponding reference compound; in c) the reference spectrum of copper decanoate is presented (blue trace).

4.2 Electrochemical measurements

4.2.1 Open circuit potentials

Open circuit potential responses for bare copper and naturally corroded samples, both untreated and treated with the various inhibitors, were recorded in the synthetic acid rain and typical potential/time profiles obtained are shown in Figure 7. In all cases, stable OCP values, shown in Tables 2 and 3, were achieved within approximately one hour of immersion of the samples in the solution.

For the untreated bare copper sample, a constant potential value of 54 mV (Table 2) was quickly reached. This could be due to the deposition of passivating corrosion products on the copper surface which occurred shortly after immersion of the sample in the solution. The OCP profiles for the inhibitor-treated samples shifted significantly becoming either more positive, for the BTA-treated sample, or more negative, for both HC10- and NaC10-treated samples, conceivably due to a layer of the inhibitors adsorbed on the active corrosion sites of the copper. By comparing the final OCP values of the untreated and treated bare copper samples, according to the classification given in [30], BTA could be classified as a mixed-type inhibitor with a predominant effect on the anodic reaction [31]. In fact, the OCP displacement in the inhibiting medium, compared to that in the uninhibited one, is less than 85 mV [30,31].

The OCP profiles obtained for the naturally corroded copper samples (Figure 7b) were somewhat noisy, probably due to the porous nature of the corrosion layers. The OCP values (Table 3) were located positively with respect to the corresponding bare copper specimens, except for BTA. These results indicated that the corrosion layers themselves protected, to some extent, the underlying metallic copper from further corrosion. In addition, based on the above considerations, for the corroded samples, all organic compounds acted as mixed-type inhibitors [30], but for HC10 with a more pronounced effect on the cathodic reaction (e.g., inhibition of the oxygen reduction process), compared to other compounds.

Figure 7: OCP profiles obtained in synthetic acid rain with (a) bare copper samples and (b) real corroded samples, untreated (black line) and treated with BTA (green line), HC10 (red line) and NaC10 (blue line).

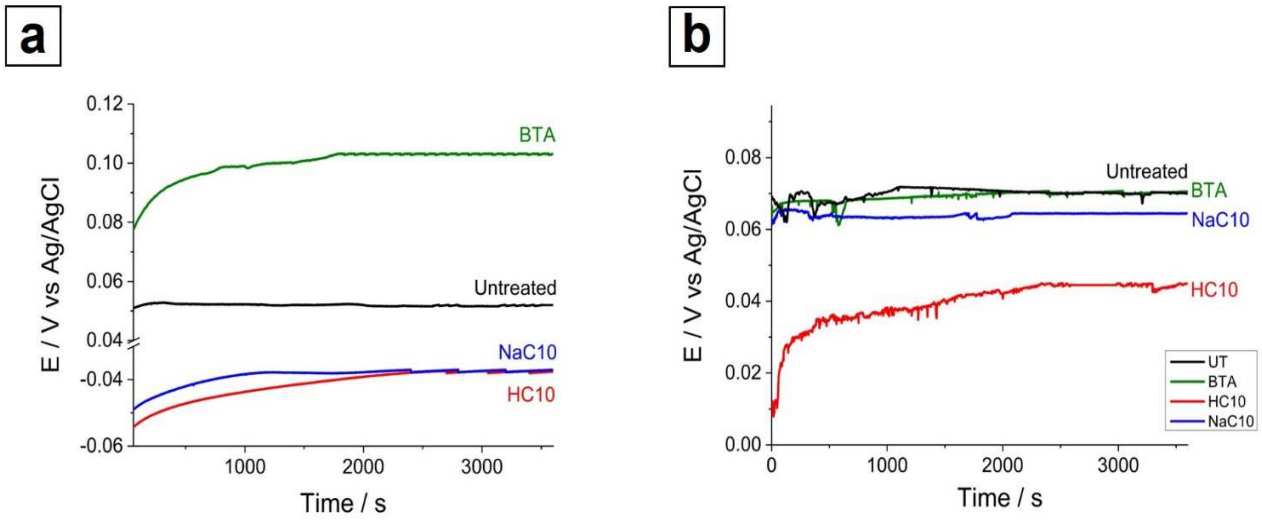

4.2.2 Potentiodynamic polarization measurements

The performances of each treatment on both bare copper and naturally corroded copper samples were evaluated by performing PDP measurements after 24 hours immersion in synthetic acid rain solution. Figure 8 shows typical PDP curves thus obtained, while Tables 2 and 3 include the associated electrochemical parameters: corrosion potentials (E_{corr}), corrosion current density (I_{corr}) and inhibition

efficiency (*IE%*). The latter was evaluated by using equation (2). Data shown in Tables 2 and 3 are average values obtained from three different specimens of the same sample immersed in the same test solutions.

Table 2: Electrochemical parameters for bare copper samples untreated and treated with the various investigated inhibitors

	OCP (mV)	***E_{corr} (mV)***	***I_{corr} (μA cm^{-2})***	***IE%***
Untreated	54 ± 3	45 ± 2	6.92 ± 0.2	
BTA	111 ± 3	107 ± 5	0.022 ± 0.005	**99.7**
HC10	-41 ± 2	-51 ± 3	0.28 ± 0.01	**92.8**
NaC10	-39 ± 3	-49 ± 4	0.29 ± 1.31	**92.5**

Table 3: Electrochemical parameters for naturally corroded samples untreated and treated with the various investigated inhibitors

	OCP (mV)	***E_{corr} (mV)***	***I_{corr} (μA cm^{-2})***	***IE%***
Untreated	66 ± 2	51 ± 2	2.38±0.07	**65.6 ***
BTA	66 ± 2	56 ± 3	0.032±0.002	**98.8**
HC10	43 ± 3	39 ± 2	0.14 ±0.01	**94.2**
NaC10	62 ± 2	48 ± 3	0.84 ±0.03	**66.2**

*The *IE%* was evaluated considering $I_{corrUT,}$ as the value obtained from the bare copper sample (i.e., Table 2, third entry).

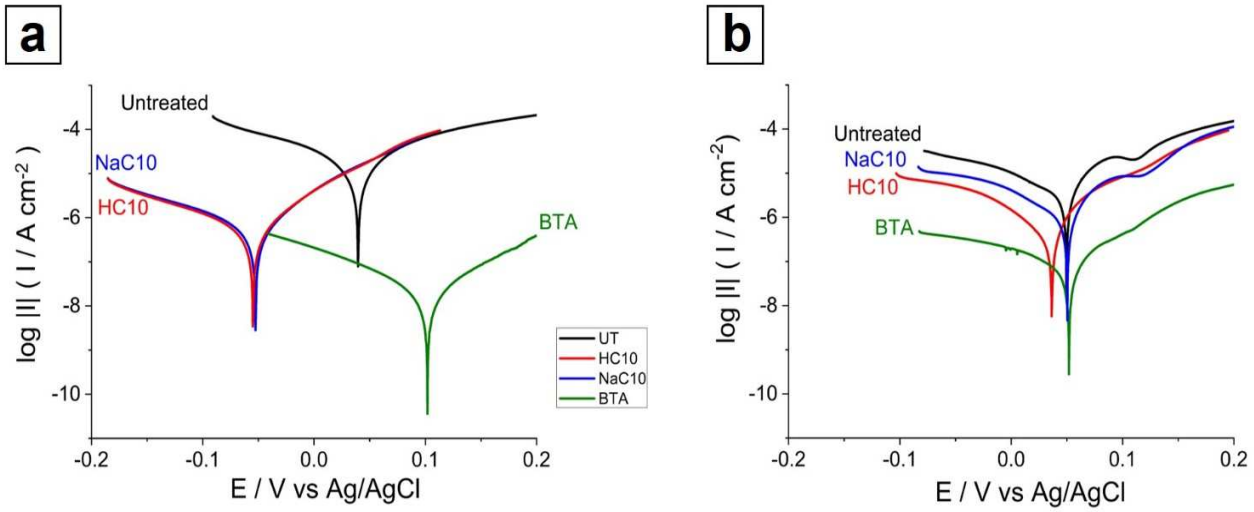

Figure 8: Typical potentiodynamic curves obtained for (a) bare copper and (b) real corroded samples either untreated or treated with BTA, HC10 and NaC10, as indicated, in acid rain.

All polarization curves recorded for the copper samples (Figure 8a) showed a regular pattern, regardless of the inhibitor employed. A drop of the corrosion current density occurred with respect to the untreated sample for both the anodic copper dissolution and cathodic reduction reactions. These results suggest that all organic compounds employed exerted a protective action against corrosion of metallic copper. However, the extent of the current decrease and, consequently, the inhibition efficiency, depended on the specific inhibitor employed, and it was the largest for BTA. This was also evident from the average *IE%* values shown in Table 2 (sixth column). The average corrosion potential shifted positively for BTA (+62 mV) and negatively for both HC10 (-96 mV) and NaC10 (-94 mV), indicating that BTA treatment predominately controlled the anodic reaction, while both HC10 and NaC10 acted as cathodic type inhibitors [30], likely preventing the occurrence of the oxygen reduction process. It must be considered that the literature reports controversial results on the effect of the

protective action of carboxylic/carboxylate compounds on copper substrates. For instance, in [14] an anodic shift of E_{corr} was observed using stearic acid. For the same carboxylic acid, a cathodic shift of E_{corr} (by a similar amount) was reported in [11, 14, 30]. In [32], a cathodic shift of E_{corr} was reported for copper in the presence of NaC10 and Na C12 (sodium dodecanoate). In some cases (e.g, in [14]), it was found that E_{corr} depended on the specific status of the substrate surface.

The values of *IE%* for BTA and HC10 found here (99.7% and 92.8%, respectively) compare to those reported in the literature for copper samples treated with the same inhibitors (i.e., *IE%* of about 98% and 90%, for BTA [33] and HC10 [14], respectively) exposed to acid rain. Concerning NaC10, the *IE%* found here is similar to that of the HC10-treated sample. To the best of our knowledge, no information is available in the literature on inhibition efficiency for NaC10-treated copper samples in acid rain. However, a pronounced copper protection was previously reported using potassium decanoate in an aqueous solution at pH 10 [34].

Considering the potentiodynamic curves recorded with the naturally corroded samples (Figure 8b) and the associated electrochemical parameters (Table 3), it was evident that the corrosion potentials of the samples treated with the inhibitors did not change significantly with respect to the untreated reference sample (i.e., not more than 13 mV). Therefore, from this perspective, it was harder to understand the predominant protection mechanism exerted by each treatment. However, corrosion currents dropped, though to a lesser extent than the corresponding bare copper samples, indicating that the investigated inhibitors, nevertheless, played a positive role in preventing corrosion of the sample in the synthetic rain solution. The apparent lower current drop was due to the fact that the already existing corrosion layer on the historical samples itself exerted a protective effect against corrosion of the underlying metallic copper. The *IE%* of the untreated corroded sample (Table 3, sixth entry), calculated by using as I_{corrUT} the value of the untreated bare copper sample (Table 2, third entry), was equal to 65.6%. With respect to the untreated corroded sample, the *IE%* obtained for BTA-treated and HC10-treated naturally

corroded samples were considerably higher (98.8% and 94%, respectively), indicating the high stability of the treatment after 24 hours in acid rain. The lower *IE%* of the NaC10-treated sample (i.e., 66.2%) could be due to the stability of the decanoate complex present on the sample surface when it is immersed in the synthetic acid rain at pH=3.1. In fact, it is known that the solubility of copper decanoate in acidic media is not negligible [35]. In addition, as stated above, NaC10 on the sample surface was, probably, only partially chemically bound. Therefore, the physical adsorbed amounts could be easily released in the acid rain.

Another specific feature of the potentiodynamic curves of the corroded samples was the presence of a double current plateau in the anodic region, the first occurring in the potential range from about 0.1 to 0.12 V. At higher potentials, the anodic current profiles increased and, for the samples treated with HC10 and NaC10, tended to overlap with that of the untreated one. The above described behavior could be related to the fact that at a potential slightly positive to E_{corr}, the oxidation of the underlying metallic copper led to the growth of a thicker passive Cu_2O layer, which at higher overpotentials oxidizes to $Cu(OH)_2$ and into the formation of an insoluble layer of Cu(II)-carboxylate.

4.3.3 Considerations regarding the passivation mechanism of the samples

From the above electrochemical measurements some conclusions can be drawn about the inhibition mechanisms involved for the corroded samples, which conceivably follow similar schemes as those described in the literature for bare copper [14, 34], apart from the direct metal oxidation steps.

The corrosion mechanism of copper in acid rain has been reported in earlier articles [14,34]. It was found that it depends on the pH and the complexing species, such as Cl^- ions, present in the medium [36]. In particular, it was reported that at pH ≥ 3.5, the rate determining step of corrosion implied a film formation/dissolution process [14, 34] involving the formation of insoluble CuCl, Cu_2O and, in aerated media, CuO or $Cu(OH)_2$ compounds. For the Cl^- concentration and pH 3.1 (i.e, conditions of the acid

rain used here), the formation of copper oxides on the copper surface should prevail, while the film dissolution due the Cl^-, to form soluble $CuCl_2^-$, should be negligible [14, 34]. In the presence of the inhibitors, passivating hydrophobic layers were formed, consisting, conceivably of either Cu(I) or Cu(II) complexes containing BTA [11] or HC10 (or $C10^-$) [14, 37]. Therefore, the formation of the hydrophobic layers on the corroded samples, which markedly decreased the wettability of their surfaces, impeded the aggressive species present in acid rain from reaching, and then destroying, either the patina layer, or the underlying metal surface.

5. Discussion

The results reported above allow highlighting additional considerations. From the PDP curves, it appears that bare copper and naturally corroded copper have different responses to corrosion in the synthetic artificial rain solution. In particular, the naturally corroded copper exhibited a lower current density, with respect to the uncorroded copper, with an inhibition efficiency, *IE%* of 65%. This is consistent with the literature [5] and is related to the presence of a protective corrosion layer that induces a decrease of the corrosion rate. The previously described corrosion layer [22], composed of an external layer of brochantite (45-50 μm thick), and cuprite (5-10 μm thick) at the interface with the metal, reflects the typical composition of long-term corroded copper samples in urban environments [4, 5]. Since the brochantite layer is porous, the protective effect is explained by the presence of cuprite in contact with the metal, which causes passivation of the copper substrate and controls the corrosion reactions.

The use of BTA to treat bare copper resulted in the inhibition of corrosion reactions (i.e., in general the current density was reduced). The anodic role of BTA can be explained by the adsorption (chemisorption and/or physisorption) of the molecules on the surface during the treatment, thus blocking the anodic dissolution of the metal. The corroded samples treated with BTA displayed a

substantial current density decrease, compared to the untreated sample, although no specific tendency could be inferred about which anodic or cathodic reaction predominated. As shown by Raman spectroscopy, the treatment on the naturally corroded copper led to the formation of a BTA-Cu complex on the surface and, as pointed out in a previous study [28], the complexation seemed to take place within the entire brochantite layer. This surface complex, insoluble in water, is responsible for the color change of the surface and for increasing surface tension.

The use of HC10 and NaC10 for the treatment of bare copper samples provides a substantial reduction of current density, compared to the untreated samples. In addition, from the PDP tests, it appeared that both inhibitors mainly affected the cathodic reactions. HC10 also displayed similar effects when employed for the treatment of naturally corroded samples. The barrier effect prevails (shift to lower potentials) due to the formation of copper decanoate crystals on the surface as observed by SEM and Raman spectroscopy. The copper decanoate crystals increased the hydrophobic properties evidenced by contact angle measurements. On the contrary, very low protective effect and no barrier effect were found for the naturally corroded sample treated with NaC10 despite the obvious modification of the surface by the treatment, as observed by SEM. The precipitate had a different morphology compared to the one observed after HC10 treatment. The chemical structure of the compound formed onto the substrate surface was also unclear compared to the copper decanoate identified when HC10 was employed: possibly an amorphous or a lower amount of crystalline copper decanoate was present after the treatment with NaC10. This could be related to the slight basicity of the hydroalcoholic solution (pH 8) containing 0.15 M of NaC10 inhibitor. Under these conditions, the amount of Cu^{2+} ions coming from dissolution of brochantite was lower than with the acidic form (pH 3.6 for 0.17 M HC10), therefore, reducing the amount of Cu^{2+} ions and NaC10 species that can form at the solid / solution interface. It can be concluded that in the case of NaC10, a protective surface layer does form right after the sample treatment (as evidenced by the surface tension measurements) but it is not stable after 24

hours immersion in the synthetic acid rain, as shown by the low protective effect of NaC10. Sodium carboxylates were also employed as inhibitors in acidic media for other metallic compounds, such as steel, providing some controversial results. In Ref. [38] sodium octanoate (NaC8) and sodium dodecanoate (NaC12) were studied as corrosion inhibitors for X60 steel in 0.5 M HCl solution. Experimental results indicated that the two alkyl carboxylates acted as corrosion inhibitors to a different extent. NaC8 exhibited better corrosion inhibition behavior (*IE*% of about 85 %), compared to that of NaC12 (*IE*% of about 20%), which also depended on the inhibitor concentration. In Ref. [39], it was shown that sodium caprylate acted as a good corrosion inhibitor for carbon steel in sulfuric acid solution, yielding a maximum corrosion inhibition efficiency of about 77%. These facts indicate that the effects of these compounds in the inhibition efficiency depend on many factors, including the nature of the materials to be treated, their surface status and the conditions under which the treatments are performed.

6. Conclusions

In this study, the protective action of two eco-friendly inhibitors, HC10 and NaC10, on copper-based artworks was investigated and compared with that of the classical inhibitor BTA with toxic properties.

. The samples tested came from the roof cladding of St Martin's Church in Metz (France), which had been exposed to long-term (>100 years) atmospheric corrosion. The effects of the various inhibitors on the naturally-formed corrosion layers (composed of brochantite, 45-50 µm thick, and a thin internal layer of cuprite 5 µm thick) were compared with those obtained from bare copper samples. The investigation was conducted using a set of complementary spectroscopic, surface analysis and electrochemical techniques. The efficacy of the inhibitors in preventing corrosion was evaluated in synthetic acid rain (pH 3.1). The results obtained indicate that the HC10 treatment is efficient in preventing corrosion for both bare copper and naturally corroded materials. This was verified by

potentiodynamic measurements which demonstrated an inhibition efficiency higher than 90%. This highly protective effect is related to the formation of a highly hydrophobic copper decanoate film on the sample surface, with a crystalline structure that was clearly documented by contact angle, SEM and Raman spectroscopy measurements. However, the formed layer was responsible for a color alteration, from pale green to a blue hue. NaC10 proved efficient when applied to bare copper (inhibition efficiency higher than 90%, obtained by PDP), whereas it was less effective on the naturally corroded materials (inhibition efficiency around 60%, obtained by PDP), despite the fact that on the latter material a hydrophobic layer with no significant color change was established by contact angle and colorimetric measurements. The lower stability of the hydrophobic layer formed using NaC10 in the synthetic acid rain could be related to the different morphology of the surface layer, for which a low crystallinity is hypothesized, as evidenced by SEM and Raman spectroscopy analysis.

Overall, the results obtained in this study demonstrate that HC10 may present a safe, eco-friendly and efficient alternative to the use of BTA as protection coating in order to maintain the naturally formed patinas of copper-based artworks exposed outdoors.

Acknowledgements

Authors would like to thank the Laboratoire de Recherche des Monuments Historique (LRMH) for providing the corroded copper sample of St Martin's Church in Metz and for their generous advice on the study.

Data availability statement

The raw/processed data required to reproduce these findings cannot be shared at this time due to technical or time limitations. They will be available on request.

References

[1] T. Graedel, K. Nassau, and J.P. Franey, Copper patinas formed in the atmosphere-I. Introduction, Corros. Sci. 27 (1987) 639–657. https://doi.org/10.1016/0010-938X(87)90047-3.

[2] L. Robbiola, L.-P. Hurtel, New contribution to the study of corrosion mechanisms of outdoor bronzes: characterization of the corroding surfaces of Rodin's bronzes. *Mém. Et. Scien. Revue Mét.*, 12 (1991) 809–823. ⟨hal-00538986⟩

[3] D. de la Fuente, J. Simancas, and M. Morcillo, Morphological study of 16-year patinas formed on copper in a wide range of atmospheric exposures, Corros. Sci. 50 (2008) 268–285. https://doi.org/10.1016/j.corsci.2007.05.030.

[4] K. P. FitzGerald, J. Nairn, G. Skennerton, and A. Atrens, Atmospheric corrosion of copper and the colour, structure and composition of natural patinas on copper, Corros. Sci. 48 (2006) 2480–2509. https://doi.org/10.1016/j.corsci.2005.09.011

[5] M. Morcillo, T. Chang, B. Chico, D.de la Fuente, I. Odnevall Wallinder, J.A. Jiménez, C. Leygraf, Characterisation of a centuries-old patinated copper roof tile from Queen Anne's Summer Palace in Prague, Mater. Charact. 133 (2017) 146–155. https://doi.org/10.1016/j.matchar.2017.09.034.

[6] A. Texier and A. Azéma, Métal à ciel ouvert. La sculpture métallique d'extérieur du XIXe au début du XXe siècle: identification, conservation, restauration, in Métal à ciel ouvert - 15es journées d'étude de la SFIIC - ICOMOS France (2014) 288.

[7] G. Masi, C. Josse, J. Esvan, C. Chiavari, E. Bernardi, C. Martini, M.C. Bignozzi, C. Monticelli, F. Zanotto, A. Balbo, Evaluation of the protectiveness of an organosilane coating on patinated Cu-Si-Mn bronze for contemporary art, Prog. Org. Coatings 127 (2019) 286–299. https://doi.org/10.1016/j.porgcoat.2018.11.027.

[8] T. Kosec, L. Škrlep, E.Š. Fabjan, A.S. Škapin, G. Masi, E. Bernardi, C. Chiavari, C. Josse, J. Esvan, L. Robbiola, Development of multi-component fluoropolymer based coating on simulated outdoor patina on quaternary bronze, Prog. Org. Coatings 131 (2019) 27–35. https://doi.org/10.1016/j.porgcoat.2019.01.040.

[9] H. Brinch Madsen, A Preliminary Note on the use of benzotriazole for stabilizing bronze objects, Stud. Conserv. 12 (1967) 163–167. https://doi.org/10.2307/1505414.

[10] L.B. Brostoff, T.J. Shedlosky, and E.R. de la Rie, External reflection study of copper-benzotriazole films on bronze in relation to pretreatments of coated outdoor bronzes, Stud. Conserv. 45 (2000) 29–33. https://doi.org/10.1179/sic.2000.45.

[11] M. Finšgar and I. Milošev, Inhibition of copper corrosion by 1, 2, 3-benzotriazole: a review, Corros. Sci. 52 (2010) 2737–2749.https://doi.org/10.1016/j.corsci.2010.05.002.

[12] X. Wu, N. Chou, D. Lupher, and L. C. Davis, Benzotriazoles: toxicity and degradation, Conf. Hazard. Waste Res. (1998) 374–382.

[13] E. Rocca, G. Bertrand, C. Rapin, and J. C. Labrune, Inhibition of copper aqueous corrosion by non-toxic linear sodium heptanoate: mechanism and ECAFM study, J. Electroanal. Chem. 503

(2001) 133–140. https://doi.org/10.1016/S0022-0728(01)00384-9.

[14] G. Žerjav and I. Milošev, Carboxylic acids as corrosion inhibitors for Cu, Zn and brasses in simulated urban rain, Int. J. Electrochem. Sci. 9 (2014) 2696–2715.

[15] E. Apchain, D. Neff, J.P. Gallien, N. Nuns, P. Berger, A. Noumowé, P. Dillmann, Efficiency and durability of protective treatments on cultural heritage copper corrosion layers, Corros. Sci. 183, (2021) 109319. https://doi.org/10.1016/j.corsci.2021.109319.

[16] M. L'héronde, M. Bouttemy, F. Mercier-Bion, D. Neff, E. Apchain, A. Etcheberry and P. Dillmann, Multiscale study of interactions between corrosion products layer formed on heritage Cu objects and organic protection treatments, Heritage 2 (2019) 2640–2651. https://doi.org/10.3390/heritage2030162.

[17] G. Brunoro, A. Frignani, A. Colledan, and C. Chiavari, Organic films for protection of copper and bronze against acid rain corrosion, Corros. Sci. 45 (2003) 2219–2231. https://doi.org/10.1016/S0010-938X(03)00065-9.

[18] D.A. Scott, Copper and Bronze in Art: Corrosion, Colorants, Conservation, J Paul Getty Museum Pubns 2002.

[19] S. Hollner, F. Mirambet, E. Rocca, and S. Reguer, Evaluation of new non-toxic corrosion inhibitors for conservation of iron artefacts, Corros. Eng. Sci. Technol. 45 (2010) 362–366. https://doi.org/10.1179/147842210X12732285051311.

[20] CIE 1976 L*a*b*Color Space, Commission Internationale de L'Eclairage, CIE Central Bureau: Vienna, Austria, 2007.

[21] R.B. Faltermeier, A Corrosion Inhibitor test for copper-based artifacts, Stud. Conserv. 44 (1998) 121–128. https://doi.org/10.1179/sic.1999.44.2.121.

[22] S. Wang, L. Feng, and L. Jiang, One-step solution-immersion process for the fabrication of stable bionic superhydrophobic surfaces, Adv. Mater. 18 (2006) 767–770. https://doi.org/10.1002/adma.200501794.

[23] S. Wang, K. Liu, X. Yao, and L. Jiang, Bioinspired surfaces with superwettability: new insight on theory, design, and applications, Chem. Rev. 2015, 115, 16, 8230–8293. https://doi.org/10.1021/cr400083y.

[24] V. Hayez, V. Costa, J. Guillaume, H. Terryn, and A. Hubin, Micro Raman spectroscopy used for the study of corrosion products on copper alloys: study of the chemical composition of artificial patinas used for restoration purposes, Analyst 130 (2005) 550-556. https://doi.org/10.1039/B419080G.

[25] A. Krätschmer, I. Odnevall Wallinder, and C. Leygraf, The evolution of outdoor copper patina, Corros. Sci. 2002, 44, 3, 425–450.

[26] E. Ferrari, D. Neff, and E. Apchain, Assessing the interaction between corrosion inhibitors and the historical corrosion layer on copper claddings based on global and micrometric-scale analysis, in Metal 2019 - Proceedings of the Interim Meeting of the ICOM-CC Metals Working Group; Neuchatel (CH), 2-6 September 2019, (2019).

[27] A. Kokalj, S. Peljhan, M. Finsgar, I. Milosev, What Determines the inhibition effectiveness of

ATA, BTAH, and BTAOH corrosion inhibitors on copper? J. Am. Chem Soc. 132 (2010) 16657 - 16668. https://doi.org/10.1021/ja107704y.

[28] T. Kosec, A. Legat, and P. Ropret, Raman investigation of artificial patinas on recent bronze protected by different azole type inhibitors in an outdoor environment, J. Raman Spectrosc. 45 (2014) 1085–1092. https://doi.org/10.1002/jrs.4532.

[29] L. Robinet and M. C. Corbeil, The characterization of metal soaps, Stud. Conserv. 48 (2003) 23–40. https://doi.org/10.1179/sic.2003.48.1.23.

[30] O. L. Riggs Jr., Corrosion Inhibitors, second ed., C.C. Nathan, Houston, 1973.

[31] I. Milošev, T. Kosec, M. Bele, The formation of hydrophobic and corrosion resistant surfaces on copper and bronze by treatment in myristic acid. J. Appl. Electrochem. 40 (2010) 1317–1323.

[32] A. Elia, K. De Wael, M. Dowsett, A. Adriaens, J. Solid. State Electrochem. 16 (2012) 143-148. DOI 10.1007/s10800-010-0078-x

[33] G. Žerjav, A. Lanzutti, F. Andreatta, L. Fedrizzi, and I. Milošev, Characterization of self-assembled layers made with stearic acid, benzotriazole, or 2-mercaptobenzimidazole on surface of copper for corrosion protection in simulated urban rain, Mater. Corros. 68 (2017) 30–41. https://doi.org/10.1002/maco.201608954.

[34] E. Abelev, D. Starosvetsky, and Y. Ein-Eli, Enhanced copper surface protection in aqueous solutions containing short-chain alkanoic acid potassium salts, Langmuir 23 (2007) 11281–11288. https://doi.org/10.1021/la701434e.

[35] Mauchauffee, E. Meux, M. Schneider Determination of the solubility products in water at 20 °C of 32 metallic carboxylates Ind. Eng. Chem. Res., 47 (2008) 7533-7537

[36] T. Liu, S. Chen, S. Cheng, J. Tian, X. Chang, Y. Yin, Corrosion behavior of super-hydrophobic surface on copper in seawater, Electrochimica Acta 52 (2007) 8003–8007. https://doi.org/10.1016/j.electacta.2007.06.072.

[37] S. Magaino, Corrosion rate of copper rotating-disk-electrode in simulated acid rain, Electrochim. Acta 42 (1997) 377 – 382. https://doi.org/10.1016/S0013-4686(96)00225-3.

[38] I.B. Obot, I.B. Onyeachu, N. Wazzan, A. H. Al-Amri,Theoretical and experimental investigation of two alkyl carboxylates as corrosion inhibitors for steel in acidic medium, Journal of Molecular Liquids, 279 (2019), 190-207. https://doi.org/10.1016/j.molliq.2019.01.116.

[39] G. Saad, O. Sasha, Corrosion inhibition of carbon steel in sulfuric acid by sodium caprylate, Int. J. Eng. Res. Appl. 6 (2016) 74 – 84.

Graphical Abstract